Korean J. Chem. Eng., 37(1), 65-71 (2020)
DOI: 10.1007/s11814-019-0417-5

pISSN: 0256-1115
eISSN: 1975-7220

Direct synthesis of H_2O_2 over Pd/C catalysts prepared by the incipient wetness impregnation method: Effect of heat treatment on catalytic activity

Vu Thi Thuy Hang and Young-Min Chung†

Department of Nano & Chemical Engineering, Kunsan National University,
558 Daehak-ro, Kunsan, Jeollabuk-do 54150, Korea
(*Received 15 September 2019 • accepted 30 October 2019*)

Abstract−Although various Pd/C catalysts have been applied in the direct synthesis of H_2O_2, unsatisfactory H_2O_2 yields have been achieved. We systematically investigated the effect of heat treatment on the physicochemical properties of Pd/C catalyst, and thereby on the catalytic performance in the direct synthesis of H_2O_2. Pd/C catalysts prepared by the incipient wetness method were subjected to different heat treatments and applied in H_2O_2 synthesis. The calcination temperature was found to have a key role in determining the Pd nanoparticle (NP) size; calcination at 523 K yielded highly oxidized and small Pd NPs corresponding to the sub-nano domain (1.4-2.5 nm). This Pd/C catalyst is superior not only in promoting H_2O_2 formation, but also in suppressing the subsequent unfavorable H_2O_2 decomposition and hydrogenation, which explains its excellent H_2O_2 productivity (as high as 4,443 mmol H_2O_2/g Pd·h) and selectivity (94.5%). On the other hand, the reaction performance of the Pd/C catalysts calcined at a higher temperature (673 K) or reduced under hydrogen was sharply reduced owing to the formation of larger Pd NPs or the enhancement of the metallic nature of Pd, respectively. The amount of residual Cl ion on Pd/C catalyst after heat treatment also had an impact on the catalytic activity as it affected the pH of reaction solution. These results clearly demonstrate that an efficient Pd/C catalyst can be realized by fine tuning the conditions of heat treatment during catalyst preparation.

Keywords: Direct Synthesis of H_2O_2, Pd/C, Incipient Wetness, Heat Treatment, Nanoparticle

INTRODUCTION

Industrial manufacture of H_2O_2 dates back more than a century. Nowadays, the H_2O_2 production method prevailing worldwide is the anthraquinone oxidation process (AO process) [1,2]. Unfortunately, this method is not attractive environmentally or economically; it is a complicated and high energy-demanding process, requires an excessive use of toxic organic solvents and generates undesirable wastes, and necessitates intensive concentration after production [3,4]. In this context, many efforts have been made to develop an alternative process that can overcome the drawbacks of the AO process.

Direct synthesis of H_2O_2 from H_2 and O_2 (DSHP) is one such promising alternative strategy by virtue of its simple and highly efficient reaction scheme in terms of atom economy. In the past decades, researchers have intensively explored the possibility of DSHP overcoming the drawbacks of the currently prevailing AO process and initiating a new environmentally-benign paradigm of H_2O_2 production. The realization of DSHP is especially highly anticipated in the chemical industry because the direct use of *in situ* generated H_2O_2 in selective oxidation processes, such as the epoxidation of propylene or partial oxidation of methane, will be advantageous in terms of securing process economy [5,6].

Unfortunately, DSHP is a very challenging reaction in terms of the potentially dangerous H_2/O_2 mixing issue and unfavorable thermodynamics. Therefore, numerous researchers have sought to design efficient catalysts for this transformation [7-21]. Among the various kinds of catalysts developed to date, palladium/activated carbon (Pd/C) catalysts have been most extensively studied because carbon materials have advantages such as low cost, availability, inertness, and stability in the presence of caustic additives. However, because simple Pd/C catalysts generally show low H_2O_2 yields, diverse strategies such as bimetallization [22-24], surface modification by acid treatments [25,26], or use of well-defined carbon supports [27-29] have been tested to improve the selectivity for H_2O_2 formation. An efficient Pd/C catalyst has also been prepared by selective adsorption deposition or sequential ligand exchange method [30,31].

In this work, Pd/C catalysts were prepared by the incipient wetness impregnation method followed by different heat treatments. While a number of Pd/C catalysts have been prepared in a solution via adsorption-reduction methods, systematic investigation for the effect of post-heat treatments on the catalytic activity has been limited because active metal adsorption and its reduction occurred simultaneously in the solution-based preparation method. As will be discussed, the reaction performance of the Pd/C catalyst for the DSHP reaction is highly dependent on the heat treatment conditions during catalyst preparation. Systematic characterization and test reactions revealed the critical role of the heat treatment conditions in determining the physicochemical properties of the catalyst and therefore its activity.

EXPERIMENTAL

1. Chemicals

Activated carbon was obtained from Cabot Corporation (Norit,

†To whom correspondence should be addressed.
E-mail: ymchung@kunsan.ac.kr

catalyst carrier grade). Palladium chloride ($PdCl_2$, 99.9%) and Ferroin indicator (0.1 wt% in H_2O) were purchased from Strem and Sigma-Aldrich, respectively. Cerium(IV) sulfate ($Ce(SO_4)_2$, 0.1 N standardized solution) was obtained from Merck Millipore. Hydrogen peroxide (H_2O_2, 34.5%), methanol (CH_3OH, 99.9%), and hydrochloric acid (HCl, 35-37%) were purchased from Samchun Chemicals, Korea. All chemicals were used as received without further purification.

2. Catalyst Preparation

Pd/C catalyst was prepared by incipient wetness impregnation method. For the preparation of the palladium precursor solution, $PdCl_2$ was dissolved in 0.5 M HCl solution. After stirring for 3 h for complete dissolution, the H_2PdCl_4 solution was kept away from light to prevent decomposition. Before impregnation, the pore volume of the activated carbon support was measured, and a corresponding volume of the H_2PdCl_4 solution was slowly added dropwise with thorough mixing to 1 g of activated carbon (Pd intake 2 wt%). After being stored at room temperature for 12 h, the Pd supported activated carbon was dried at 393 K for 4 h. Next, the dried sample was exposed under air to different temperatures ranging from 423 to 673 K for 3 h at a heating rate of 5 K/min. Additional reduction of the catalyst was performed in the presence of mixed N_2/H_2 gas (50 mol% H_2, 100 mL/min) at 473 K for 3 h (heating rate=5 K/min). Recalcination of the catalyst was at 525 K for 3 h under air.

3. Characterization

Powder X-ray diffraction (PXRD) analysis of the prepared samples was performed using a Malvern Panalytical Empyrean high-resolution X-ray diffractometer. X-ray photoelectron spectroscopy (XPS) analysis was carried out to investigate the binding energies of Pd in the samples using a Thermo VG Scientific MultiLab 2000 apparatus with an Al anode and 30 eV of pass energy (step increment=0.1 eV). The size of the Pd NPs and their distribution were determined by analyzing the transmission electron microscopy (TEM) images obtained using a Philips Tecnai G2 F30 transmission electron microscope. High-angle annular dark-field scanning transmission electron microscopy (HAADF-STEM) images were obtained using a Jeol JEM 2200FS field emission transmission microscope. Residual Cl content on the surface of the Pd/C catalyst was examined by energy-dispersive X-ray spectroscopy (EDS, HORIBA 7953-H).

4. Direct Synthesis of H_2O_2

The DSHP reaction was performed as previously described in the absence of any additives [30,31]. Typically, 20 mg of the catalyst and 25 g of methanol/water mixture (80 wt% MeOH) were added into a 100 mL jacketed high-pressure reactor (Büchi Picoclave, Switzerland) connected to a circulator (Julabo F25-HE, Germany). To maximize gas-liquid contact during a reaction, a turbine type impeller connected to a gassing stirrer shaft was used. After sweeping the residual gases, the reactor was filled with the mixed reactant gases ($H_2/O_2/N_2$ (vol%)=3.8/5.0/91.2) and pressurized to 30 bar using mass flow controllers. After the reactor pressure was stabilized at 275 K, the reaction was initiated with vigorous stirring (1,200 rpm) using a magnetically-driven stirrer. The reaction was maintained for 1 h or extended to 2-4 h. During the reaction, the total flow rate of the mixed gases was maintained at 40 mL/min. To investigate the change in H_2 concentration during the reaction, the off-gas was analyzed using an Agilent 6890 gas chromatograph (GC) equipped with a Carboxen-1010 PLOT capillary column and thermal conductivity detector (TCD). The H_2O_2 content was measured by titration using an acidic cerium(IV) sulfate solution and ferroin indicator. H_2 conversion and H_2O_2 selectivity were calculated based on the H_2O_2 and H_2 concentrations determined by the volumetric titration and GC analysis, respectively. The H_2O_2 productivity is defined as the amount of H_2O_2 produced per hour divided by the Pd content (mmol H_2O_2/g Pd·h).

$$H_2 \text{ Conversion } (\%) = \frac{\text{Moles of } H_2 \text{ reacted}}{\text{Moles of } H_2 \text{ supplied}} \times 100$$

$$H_2O_2 \text{ Selectivity } (\%) = \frac{\text{Moles of } H_2O_2 \text{ produced}}{\text{Moles of } H_2 \text{ reacted}} \times 100$$

5. H_2O_2 Decomposition and Hydrogenation

H_2O_2 decomposition and hydrogenation tests were performed at 275 K under atmospheric pressure using the prepared catalyst (20 mg) and 1 wt% H_2O_2 in a methanol/water mixed solution in the presence of nitrogen or hydrogen gas (10 mL/min), respectively. During the experiment, the liquid sample was periodically extracted and titrated to monitor changes in the H_2O_2 concentration.

RESULTS AND DISCUSSION

1. Catalyst Preparation and Characterization

The effect of heat treatment conditions on the performance of Pd/C catalysts for DSHP was studied using five catalysts. The Pd/C catalysts calcined at 423, 523, and 673 K were designated as Pd/C1, Pd/C2, and Pd/C3, respectively. The Pd/C2R catalyst was prepared by reduction of Pd/C2 under hydrogen, and Pd/C2RC was obtained by recalcination of Pd/C2R. The Pd/C catalysts prepared in this study are listed in Table 1.

Fig. 1 shows the high-angle annular dark field scanning transmission electron microscope (HAADF-STEM) images of the Pd/C catalysts, and changes in the Pd NP size distribution depending on the heat treatment conditions. It was found that the calcination temperature played a crucial role in determining not only the average Pd NP size but also its distribution. In the case of Pd/C2 calcined at 523 K, smaller and narrowly distributed Pd NPs were formed (2.5±1.0 nm) compared to those of Pd/C1 calcined at 423 K (5.2±1.8 nm). On the other hand, the formation of very large and polydisperse Pd NPs (22.5±3.4 nm) on Pd/C3 indicated that unwanted sintering had occurred between Pd NPs at the high temperature (673 K). The Pd NP size of Pd/C2 was slightly increased by subsequent reduction and reduction-recalcination (as large as 5.1±1.6

Table 1. Catalyst index based on heat treatment conditions

Catalyst	Heat treatment conditions, atmosphere (temperature, K)
Pd/C1	Air (423)
Pd/C2	Air (523)
Pd/C3	Air (673)
Pd/C2R	Air (523) - H_2 (473)
Pd/C2RC	Air (523) - H_2 (473) - Air (523)

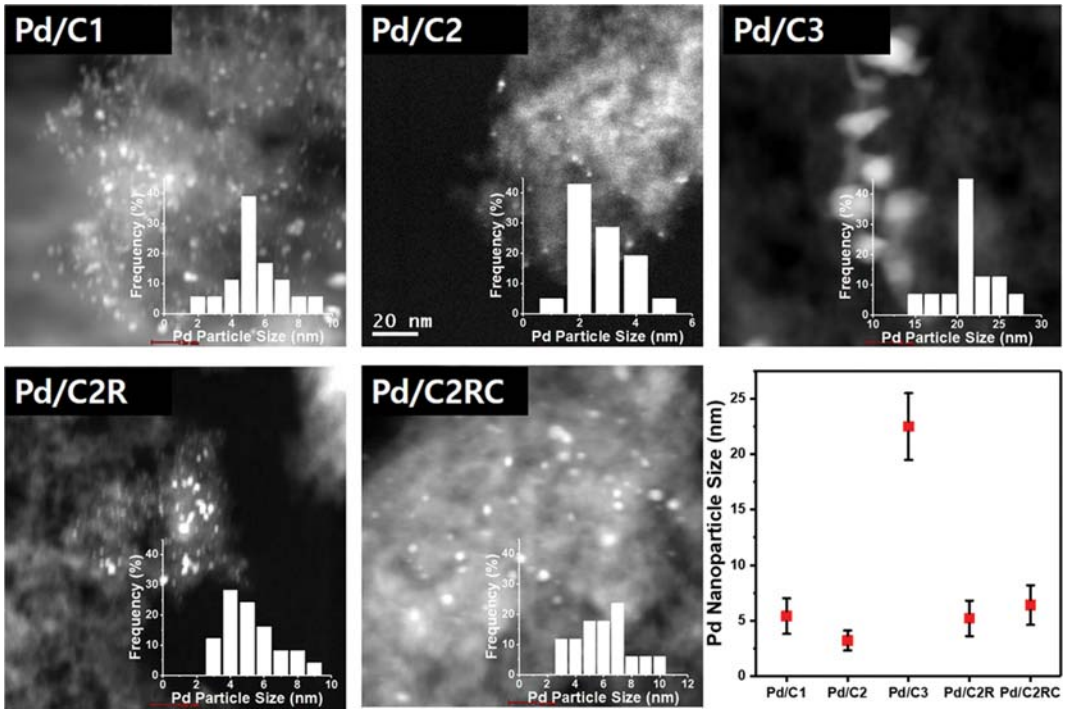

Fig. 1. HAADF-STEM images of Pd/C catalysts and Pd nanoparticle size distributions incorporated on the activated carbon support.

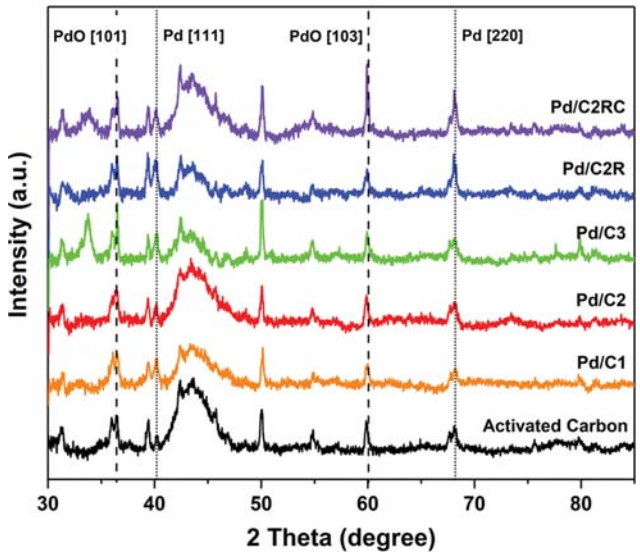

Fig. 2. PXRD patterns of Pd/C catalysts.

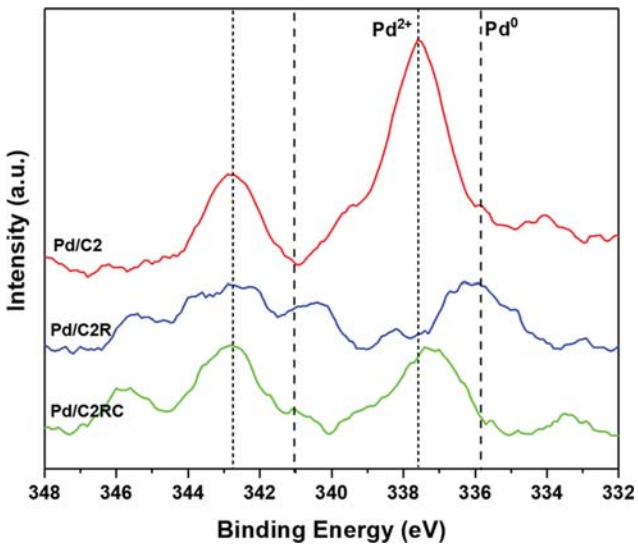

Fig. 3. Pd 3d XPS spectra of Pd/C catalysts.

nm (for Pd/C2R) and 6.2±1.0 nm (for Pd/C2RC), respectively).

The powder X-ray diffraction (PXRD) patterns of Pd/C catalysts presented in Fig. 2 indicate that there was little change in the crystallinity of Pd on altering the heat treatment conditions. However, the enhanced intensity of the PdO [101] peak at 36° (2θ) for Pd/C3 suggested that the PdO crystal could grow in the [101] direction as the temperature increased. Moreover, the strong PdO [103] peak of Pd/C2RC suggested that palladium was oxidized again upon re-calcination.

The changes in the oxidation state of Pd on reduction and recalcination were investigated by XPS analysis (Fig. 3). In the case of Pd/C2, the strong Pd $3d_{5/2}$ peak at 337.6 eV and Pd $3d_{3/2}$ peak at 342.8 eV corresponding to Pd^{2+} indicated that most Pd existed as Pd^{2+} or PdO after calcination at 523 K [32,33]. After reduction (Pd/C2R), however, the characteristic peaks for Pd^{2+} completely disappeared and new peaks for Pd^0 (336 eV for Pd $3d_{5/2}$ and 340.2 eV for Pd $3d_{3/2}$) could be observed, suggesting that the metallic nature of Pd was greatly enhanced on H_2 reduction. On the other hand, reappearance of the peaks corresponding to Pd^{2+} in the XPS analysis of Pd/C2RC implied that the metallic Pd on Pd/C2R catalyst could be fully re-oxidized by recalcination, although the Pd NP size was

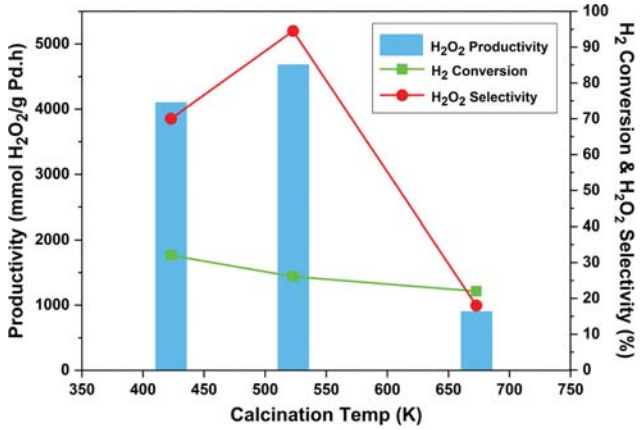

Fig. 4. Effect of calcination temperature on the reaction performance of Pd/C catalyst in the direct synthesis of H_2O_2.

slightly increased (see Fig. 1).

2. Direct Synthesis, Decomposition, and Hydrogenation Reaction of H_2O_2

The DSHP reaction was performed in the presence of a series of Pd/C catalysts calcined at different temperatures. As presented in Fig. 4, the calcination temperature had a considerable influence on the catalytic activity of Pd/C. The volcano-type changes observed in H_2O_2 productivity and selectivity strongly suggested that fine-tuning of the calcination temperature was of prime importance in realizing an efficient Pd/C catalyst for the DSHP reaction. It was found that the Pd/C2 catalyst calcined at 523 K showed superior activity, and the initial H_2O_2 productivity and selectivity reached as high as 4,443 mmol H_2O_2/g Pd.h and 94.5%, respectively. However, H_2O_2 productivity and selectivity were sharply reduced in the presence of Pd/C3 catalyst calcined at 673 K. Further, H_2 conversion gradually decreased as the calcination temperature increased.

Fig. 5 clearly indicates that not only H_2O_2 productivity but also selectivity decreased with increasing Pd NP size in the Pd/C catalysts. The inverse relationship between the Pd NP size and H_2O_2 productivity/selectivity implied that smaller Pd NPs were superior and enhanced the formation of H_2O_2. However, highly dispersed Pd or smaller Pd NP size are not always beneficial for the DSHP reaction. Han and coworkers reported that there is an optimal range of Pd NP sizes in which a certain palladium phase that is selective for H_2O_2 formation is preferentially exposed [34,35]. According to their classification, Pd NP sizes ranging from 1.4 to 2.5 nm (sub-nano domain) were particularly advantageous for selective H_2O_2 formation. Too small Pd NPs or single site Pd with sizes below the sub-nano domain were less effective in improving H_2O_2 yield. On the other hand, within the nano domain (Pd NP size >5 nm), the effect of Pd NP size on the formation of H_2O_2 became non-negligible. Similar particle size effects on catalytic performances have been reported elsewhere [30,36].

In this context, the excellent reaction performance of the Pd/C2 catalyst can be understood in terms of the Pd NP size. That is, the Pd NP size of Pd/C2 catalyst corresponding to the sub-nano domain played a role in maximizing H_2O_2 formation. Considering that the Pd NP sizes of both Pd/C1 and Pd/C3 catalysts were in the nano domain, the poor reaction performance of the Pd/C3 catalyst implies that there was another factor that influenced the catalysis. While it is reasonable to consider that the electronic nature of Pd could also affect the catalytic activity, XPS analysis of the Pd/C*x* catalysts (where *x*=1-3) indicated that most Pd existed as Pd^{2+} regardless of the calcination temperature (Fig. 3).

To investigate the effect of the electronic nature of Pd on the reaction performance, the Pd/C2 catalyst was reduced, and the catalytic activity of the resulting Pd/C2R catalyst was evaluated. As shown in Fig. 6, the additional reduction increased H_2 conversion at the expense of a steep reduction in H_2O_2 selectivity. This result strongly suggests that the electronic nature of Pd NP is as important as its size in determining the catalytic activity of Pd/C for the DSHP reaction, and the considerably decreased H_2O_2 yield was attributed to the enhanced metallic nature of Pd by H_2 reduction. The slightly enlarged Pd NPs of the Pd/C2R catalyst were also unfavorable for the formation of H_2O_2. Rebounded H_2O_2 selectivity in the presence of the re-calcined Pd/C2RC catalyst confirmed that oxidized Pd increased H_2O_2 yield. However, although the metallic Pd was easily re-oxidized by recalcination (Fig. 3), the activity of Pd/C2 catalyst was hardly recovered. The inferior activity of the Pd/

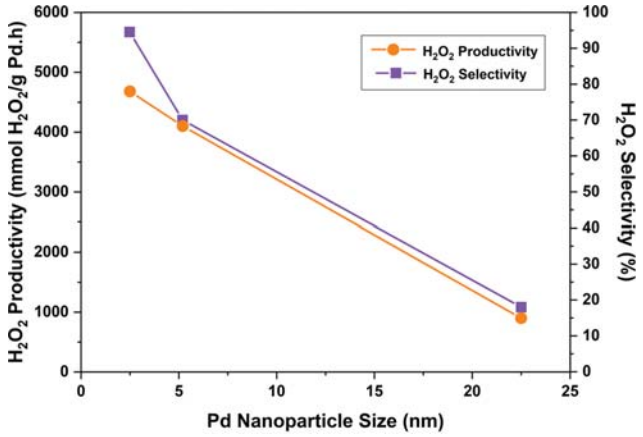

Fig. 5. Effect of Pd nanoparticle size of Pd/C catalyst on H_2O_2 productivity and selectivity.

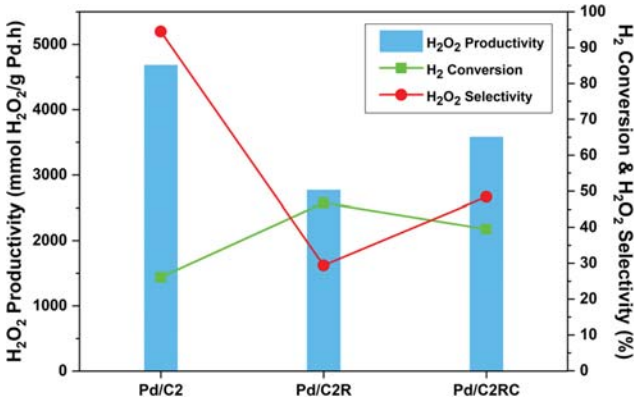

Fig. 6. Changes in the reaction performances of Pd/C catalyst depending on the post heat treatment conditions.

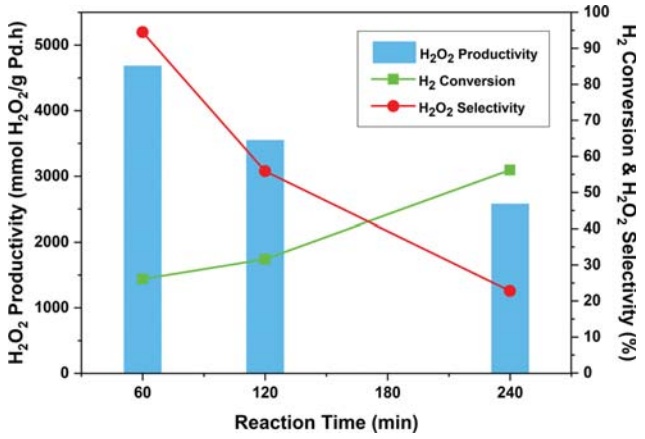

Fig. 7. Changes in time-dependent activity of the Pd/C2 catalyst in the direct synthesis of H_2O_2.

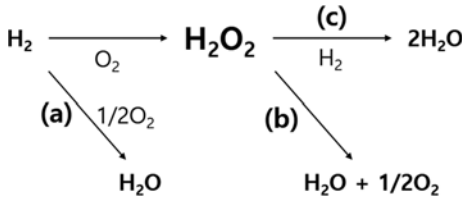

Scheme 1. Reaction pathways related to the direct synthesis of H_2O_2 from H_2 and O_2: (a) H_2 oxidation, (b) H_2O_2 decomposition, and (c) H_2O_2 hydrogenation.

C2RC might be due to the enlarged Pd NP size after recalcination (6.2±1.0 nm) compared to that of Pd/C2 (2.5±1.0 nm), which also indicated the important role of Pd NP size on the catalytic performance.

Fig. 7 shows the time-dependent changes in H_2O_2 productivity, H_2 conversion, and H_2O_2 selectivity during the DSHP reaction in the presence of the Pd/C2 catalyst. Both H_2O_2 productivity and selectivity significantly decreased with increasing reaction time. The gradual decrease in the H_2O_2 yield during the reaction indicated that the active metal Pd not only catalyzed the formation of H_2O_2 but also the subsequent H_2O_2 decomposition and hydrogenation reaction, and the non-selective oxidation of H_2 to H_2O, as described in Scheme 1. Thus, the increase in H_2 conversion with time could be explained by the additional participation of H_2 in the H_2O_2 hydrogenation reaction, as well as in the direct synthesis of H_2O_2.

Moreover, the reduced reaction performance of the Pd/C2 catalyst in the extended run might also be ascribed to the gradual decrease in the catalyst stability caused by the changes in the oxidation state of Pd. In the absence of a second metal capable of inducing a permanent oxidation of Pd, Pd might have been gradually reduced under the relatively low oxygen partial pressure, which resulted in the loss of activity. Improvement of catalyst stability under excessive oxygen condition was also reported elsewhere [37,38].

Because all the reaction pathways shown in Scheme 1 are thermodynamically favorable and can be promoted by Pd, the reaction performance of a catalyst for the DSHP may be determined by the combination of not only the H_2O_2 formation activity but also the subsequent H_2O_2 decomposition and hydrogenation activities. Thus, H_2O_2 decomposition and hydrogenation were carried out in the presence of the synthesized Pd/C catalysts. As shown in Fig. 8, the heat treatment conditions during catalyst preparation exerted a crucial effect on the degree of H_2O_2 decomposition and hydrogenation. Compared to Pd/C1 and Pd/C2, the Pd/C3 catalyst accelerated both H_2O_2 decomposition and hydrogenation rates, which indicated that larger Pd NPs preferentially promoted the undesirable side-reactions and resulted in poor H_2O_2 yield in the DSHP reaction [26,30,34]. The higher H_2O_2 decomposition and hydrogenation rates in the presence of Pd/C2R also indicated that the enhanced metallic nature of Pd was responsible for the reduced H_2O_2 yield in the DSHP reaction. The suppression of the unfavorable side-reactions by recalcination closely matched the partially recovered H_2O_2 selectivity in the DSHP reaction using the recalcined Pd/C2RC catalyst (see Fig. 6).

3. Effect of Residual Cl on the Catalytic Activity

Since the palladium precursor ($PdCl_2$) contains chloride ions that may affect the catalytic activity by suppressing H_2O_2 decomposition and by poisoning unselective sites of Pd [3], the variations in the amount of residual Cl ion and pH of the reaction solution due to changes in the heat treatment conditions were investigated. As

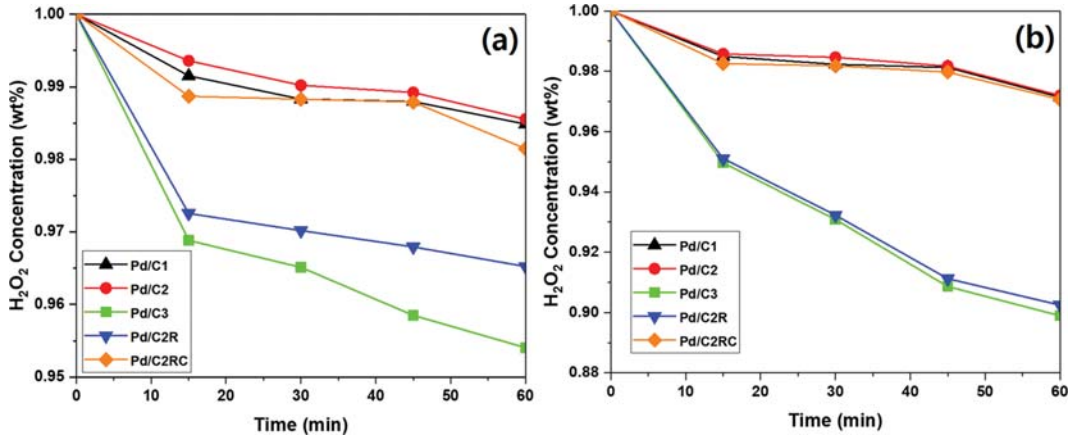

Fig. 8. (a) H_2O_2 decomposition and (b) H_2O_2 hydrogenation over Pd/C catalysts.

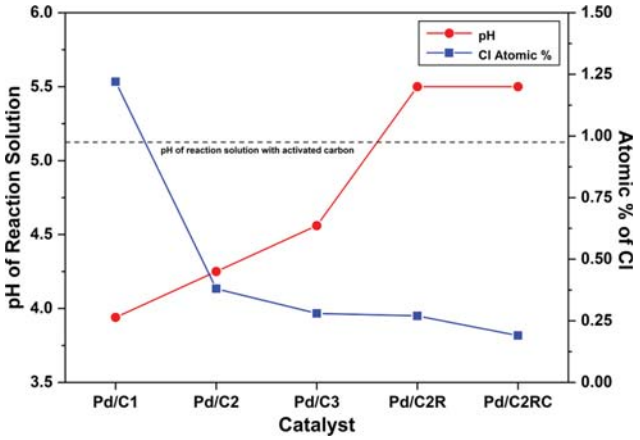

Fig. 9. Effect of residual Cl ion on the pH of the catalytic reaction solution.

revealed in Fig. 9, the residual Cl content decreased as the calcination temperature increased, and subsequent heat treatments were performed. The high Cl content of Pd/C1 (~1.25 at%) indicated that the calcination temperature (423 K) was too low to efficiently decompose the Cl ion. While its concentration decreased considerably after calcination above 523 K, residual Cl ion was found regardless of the heat treatment conditions.

The pH of the reaction solution decreased with increasing Cl ion content in the catalyst, indicating that the residual Cl ions were responsible for increasing the concentration of protons in the reaction solution. The increase in proton concentration was clearly efficient in suppressing the undesirable H_2O_2 decomposition to HO_2^- and H^+ [3,4]. Therefore, the superior reaction performance of Pd/C2 catalyst might be partially attributed to the increased proton concentration in the reaction solution by the residual Cl ion. On the other hand, the higher pH of the reaction solution after reduction suggests that the amount of Cl ions enabling proton generation decreased upon reduction. These results clearly imply that the heat treatment conditions played a crucial role in determining the reaction performance of the Pd/C catalyst by affecting the pH of the reaction solution and changing the physicochemical properties of the Pd NPs.

CONCLUSION

Pd/C catalysts were prepared by the incipient wetness impregnation method, and the effect of heat treatment conditions on the catalytic activity in the direct synthesis of H_2O_2 was investigated. The heat treatment conditions exerted considerable influence not only on the H_2O_2 formation activity but also on the subsequent H_2O_2 decomposition and hydrogenation activity of the Pd/C catalyst by affecting the nanoparticle size and the electronic nature of Pd. Furthermore, the lower pH of the reaction solution with increasing Cl content on the Pd/C catalyst implied that the residual Cl ion affected the catalytic activity by increasing the proton concentration in the reaction solution. The Pd/C catalyst calcined at 523 K achieved promising H_2O_2 productivity of 4,443 mmol H_2O_2/g Pd·h with 94.5% selectivity, which was attributed to the formation of highly oxidized, small Pd NPs (sub-nano sizes of 1.4-2.5 nm). This promising activity clearly demonstrates that the reaction performance of the Pd/C catalysts can be maximized by fine tuning of the heat treatment conditions during catalyst preparation.

ACKNOWLEDGEMENT

This research was supported by Basic Science Research Program through the National Research Foundation of Korea (NRF) funded by the Ministry of Education (2016R1D1A3B02006928).

REFERENCES

1. G. Goor, J. Glenneberg and S. Jacobi, Hydrogen Peroxide in Ullmann's Encycl. Ind. Chem., Wiley-VCH Verlag GmbH, Weinheim (2012).
2. N. M. Wilson, D. T. Bregante, P. Priyadarshini and D. W. Flaherty, *Catalysis*, **29**, 122 (2017).
3. C. Samanta, *Appl. Catal. A Gen.*, **350**, 133 (2008).
4. D. W. Flaherty, *ACS Catal.*, **8**, 1520 (2018).
5. PERP Report - Propylene Oxide 02/03-8, Nexant, New York (2003).
6. M. H. Ab Rahim, M. M. Forde, R. L. Jenkins, C. Hammond, Q. He, N. Dimitratos, J. A. Lopez-Sanchez, A. F. Carley, S. H. Taylor, D. J. Willock, D. M. Murphy, C. J. Kiely and G. J. Hutchings, *Angew. Chem. Int. Ed.*, **52**, 1280 (2013).
7. N. N. Edwin, M. Piccinini, J. C. Pritchard, Q. He, J. K. Edwards, A. F. Carley, J. A. Moulijn, C. J. Kiely and G. J. Hutchings, *ChemCatChem*, **1**, 479 (2009).
8. J. K. Edwards, S. J. Freakley, A. F. Carley, C. J. Kiely and G. J. Hutchings, *Acc. Chem. Res.*, **47**, 845 (2014).
9. F. Menegazzo, M. Signoretto, E. Ghedini and G. Strukul, *Catalysts*, **9**, 251 (2019).
10. V. S. Sumanth Ranganathan, *Catalysts*, **8**, 379 (2018).
11. W. Tu, X. Li, R. Wang, H. S. Malhi, J. Ran, Y. Shi and Y.-F. Han, *J. Catal.*, **377**, 494 (2019).
12. R. J. Lewis and G. J. Hutchings, *ChemCatChem*, **11**, 298 (2019).
13. M. Selinsek, B. J. Deschner, D. E. Doronkin, T. L. Sheppard, J.-D. Grunwaldt and R. Dittmeyer, *ACS Catal.*, **8**, 2546 (2018).
14. Y. M. Chung, *Korean Chem. Eng. Res.*, **53**, 262 (2015).
15. N. M. Wilson and D. W. Flaherty, *J. Am. Chem. Soc.*, **138**, 574 (2016).
16. S. J. Freakley, Q. He, J. H. Harrhy, L. Lu, D. A. Crole, D. J. Morgan, E. N. Ntainjua, J. K. Edwards, A. F. Carley, A. Y. Borisevich, C. J. Kiely and G. J. Hutchings, *Science*, **351**, 965 (2016).
17. M. Seo, D.-W. Lee, S. S. Han and K.-Y. Lee, *ACS Catal.*, **7**, 3039 (2017).
18. M. Seo, H. J. Kim, S. S. Han and K. Y. Lee, *Catal. Surv. from Asia*, **21**, 1 (2017).
19. J. W. Lee, J. K. Kim, T. H. Kang, E. J. Lee and I. K. Song, *Catal. Today*, **293-294**, 49 (2017).
20. Y. Ye, J. Chun, S. Park, T. J. Kim, Y. M. Chung, S. H. Oh, I. K. Song and J. Lee, *Korean J. Chem. Eng.*, **29**, 1115 (2012).
21. J. S. Kim, H. K. Kim, S. H. Kim, I. Kim, T. Yu, G. H. Han, K. Y. Lee, J. C. Lee and J. P. Ahn, *ACS Nano*, **13**, 4761 (2019).
22. J. K. Edwards, N. N. Edwin, A. F. Carley, A. A. Herzing, C. J. Kiely and G. J. Hutchings, *Angew. Chem. Int. Ed.*, **48**, 8512 (2009).
23. X. Xiao, T. U. Kang, H. Nam, S. H. Bhang, S. Y. Lee, J. P. Ahn and

T. Yu, *Korean J. Chem. Eng.*, **35**, 2379 (2018).
24. Y. Jang, H. Nam, J. Song and S. Lee, *Korean J. Chem. Eng.*, **36**, 1417 (2019).
25. J. K. Edwards, B. Solsona, E. Ntainjua N, A. F. Carley, A. A. Herzing, C. J. Kiely and G. J. Hutchings, *Science*, **323**, 1037 (2009).
26. B. Hu, W. Deng, R. Li, Q. Zhang, Y. Wang, F. Delplanque-Janssens, D. Paul, F. Desmedt and P. Miquel, *J. Catal.*, **319**, 15 (2014).
27. T. García, S. Agouram, A. Dejoz, J. F. Sánchez-Royo, L. Torrente-Murciano and B. Solsona, *Catal. Today*, **248**, 48 (2015).
28. R. Arrigo, M. E. Schuster, S. Abate, G. Giorgianni, G. Centi, S. Perathoner, S. Wrabetz, V. Pfeifer, M. Antonietti and R. Schlögl, *ACS Catal.*, **6**, 6959 (2016).
29. S. Yook, H. C. Kwon, Y. G. Kim, W. Choi and M. Choi, *ACS Sustain. Chem. Eng.*, **5**, 1208 (2017).
30. S. Lee, H. Jeong and Y.-M. Chung, *J. Catal.*, **365**, 125 (2018).
31. S. Lee and Y.-M. Chung, *Mater. Lett.*, **234**, 58 (2019).
32. Y.-M. Chung, Y.-T. Kwon, T. J. Kim, S.-H. Oh and C.-S. Lee, *Chem. Commun.*, **47**, 5705 (2011).
33. J. Kim, Y.-M. Chung, S. M. Kang, C. H. Choi, B. Y. Kim, Y. T. Kwon, T. J. Kim, S. H. Oh and C. S. Lee, *ACS Catal.*, **2**, 1042 (2012).
34. P. Tian, L. Ouyang, X. Xu, C. Ao, X. Xu, R. Si, X. Shen, M. Lin, J. Xu and Y. F. Han, *J. Catal.*, **349**, 30 (2017).
35. P. Tian, D. Ding, Y. Sun, F. Xuan, X. Xu, J. Xu and Y. F. Han, *J. Catal.*, **369**, 95 (2019).
36. A. Villa, S. J. Freakley, M. Schiavoni, J. K. Edwards, C. Hammond, G. M. Veith, W. Wang, D. Wang, L. Prati, N. Dimitratos and G. J. Hutchings, *Catal. Sci. Technol.*, **6**, 694 (2016).
37. F. Menegazzo, M. Signoretto, M. Manzoli, F. Boccuzzi, G. Cruciani, F. Pinna and G. Strukul, *J. Catal.*, **268**, 122 (2009).
38. G. Bernardotto, F. Menegazzo, F. Pinna, M. Signoretto, G. Cruciani and G. Strukul, *Appl. Catal. A Gen.*, **358**, 129 (2009).